

# Hybrid integrator-gain system based integral resonant controllers for negative imaginary systems

Kanghong Shi, Ian R. Petersen, *Life Fellow, IEEE*

**Abstract**—We introduce a hybrid control system called a hybrid integrator-gain system (HIGS) based integral resonant controller (IRC) to stabilize negative imaginary (NI) systems. A HIGS-based IRC has a similar structure to an IRC, with the integrator replaced by a HIGS. We show that a HIGS-based IRC is an NI system. Also, for a SISO NI system with a minimal realization, we show there exists a HIGS-based IRC such that their closed-loop interconnection is asymptotically stable. Also, we propose a proportional-integral-double-integral resonant controller (PI<sup>2</sup>RC) and a HIGS-based PI<sup>2</sup>RC, and we show that both of them can be applied to asymptotically stabilize an NI system. An example is provided to illustrate the proposed results.

**Index Terms**—hybrid integrator-gain system, integral resonant control (IRC), negative imaginary (NI) system, stability, robust control.

## I. INTRODUCTION

Negative imaginary (NI) systems theory was introduced in [1], [2] to address the robust control problem for flexible structures [3]–[5], which usually have highly resonant dynamics. Roughly speaking, a square, real-rational and proper transfer function  $G(s)$  is said to be NI if it has no strict right-half plane poles and its frequency response  $G(j\omega)$  satisfies  $j[G(j\omega) - G(j\omega)^*] \geq 0$  for all  $\omega > 0$  [1]. Typical examples of NI systems are mechanical systems with colocated force actuators and position sensors. NI systems theory provides an alternative approach to the passivity theory [6] when velocity measurements are unavailable. In comparison to passivity theory, which can only deal with systems with a relative degree of zero or one, an advantage of NI systems theory is that it allows systems to have relative degree zero, one, and two [7]. An NI system can be stabilized using a strictly negative imaginary (SNI) controller. Under some assumptions, the positive feedback interconnection of an NI system  $G(s)$  and an SNI system  $R(s)$  is asymptotically stable if and only if the DC loop gain of the interconnection is strictly less than unity; i.e.,  $\lambda_{max}(G(0)R(0)) < 1$  (e.g., see [8]). NI systems theory has found its applications in many fields including nano-positioning [9]–[12], control of lightly damped structures [13]–[15], and control of power systems [16].

NI systems theory was extended to nonlinear systems in [17]–[19]. A nonlinear system is said to be NI if the

system is dissipative with respect to the inner product of the system input and the time derivative of the system output. Under some assumptions, a nonlinear NI system can be asymptotically stabilized using a nonlinear output strictly negative imaginary (OSNI) system. Such a nonlinear extension of NI systems theory not only makes NI systems theory applicable to a broader class of plants, but also allows the use of more advanced controllers.

One such controller is the hybrid integrator-gain system (HIGS). HIGS elements were introduced in [20] to overcome the inherent limitations of linear control systems (see e.g., [21]). A HIGS switches between an integrator mode and a gain mode in order to have a sector-bounded input-output relationship. Compared with an integrator, which has a phase lag of  $90^\circ$ , a HIGS has a similar magnitude slope but only a  $38.1^\circ$  phase lag. This  $52.9^\circ$  phase reduction can significantly reduce time delay, and as a consequence, the overshoot; see [22] for a concrete example; see also [23]–[26]. It is shown in [27] that a HIGS element is a nonlinear NI system, and can be applied as a controller to asymptotically stabilize an NI plant. The paper [28] proposes a control methodology for multi-input multi-output (MIMO) NI systems using multi-HIGS controllers. Also, [28] reports the results of a hardware experiment where a multi-HIGS is applied to improve the performance of a micro-electromechanical system (MEMS) nanopositioner. The HIGS-based control methodologies proposed in [27], [28] also motivated an NI systems theory for systems with switching [29]. In addition, based on the discrete-time NI systems theory [30], a digital control approach is proposed for NI systems [31], where discrete-time HIGS are used as controllers. Considering the effectiveness of HIGS-based control and the advantages of HIGS elements over linear integral controllers, we may naturally ask the question: rather than using a HIGS as a standalone controller, can we replace integrators with HIGS elements in more intricate controllers to enhance control performance? In this paper, we investigate this problem for a HIGS-based integral resonant controller.

IRC was introduced in [32] to provide damping control for flexible structures. For a system with transfer matrix  $G(s)$ , an IRC is implemented by first adding a direct feedthrough  $D$  to the system  $G(s)$  and then applying an integrator in positive feedback to  $G(s) + D$ . Adding such a feedthrough  $D$  changes the pole-zero interlacing of  $G(s)$  into a zero-pole interlacing in  $G(s) + D$ . It is shown in [2], [33] that an IRC is an SNI system and can stabilize systems with the NI property. Since IRC are effective in damping control and easy to implement, they have been widely applied in the control of NI systems;

This work was supported by the Australian Research Council under grant DP230102443.

K. Shi and I. R. Petersen are with the School of Engineering, College of Engineering, Computing and Cybernetics, Australian National University, Canberra, Acton, ACT 2601, Australia. K. Shi is also with the Australian Centre for Robotics, University of Sydney, NSW 2006, Australia. kanghong@ieee.org, ian.petersen@anu.edu.au.

e.g., see [34]–[36].

In this paper, we propose a HIGS-based IRC by replacing the integrator in an IRC by a HIGS element. The advantages of a HIGS-based IRC are two-fold: 1) it utilizes the advantages of a HIGS in terms of small phase lag, reduced time delay and reduced overshoot; 2) A HIGS has two parameters – the integrator frequency and gain value, while an integrator only has one parameter  $\Gamma$ . Hence, a greater degree of freedom in parameters is allowed in controller design using a HIGS-based IRC. We provide a state-space model of a HIGS-based IRC. We show that a HIGS-based IRC has the nonlinear NI property. We also show that given a SISO NI system with minimal realization, there exists a HIGS-based IRC such that their closed-loop interconnection is asymptotically stable. This is illustrated using an example.

We also investigate proportional-integral-double-integral resonant controllers (PII<sup>2</sup>RC) in this paper. A PII<sup>2</sup>RC is implemented by replacing the integrator in an IRC by a proportional-integral-double-integral controller with the transfer function  $C(s) = k_p + k_1/s + k_2/s^2$ . We show that a PII<sup>2</sup>RC is an SNI system and can asymptotically stabilize an NI plant. Then, by replacing the integrators in an PII<sup>2</sup>RC with HIGS elements, we construct a HIGS-based PII<sup>2</sup>RC. We show that a HIGS-based PII<sup>2</sup>RC can also provide asymptotic stabilization for NI plants.

The rest of the paper is organized as follows: Section II provides some preliminary results on negative imaginary systems theory, IRC and HIGS. Section III provides a model for the HIGS-based IRC and shows that it can be used in the control of NI systems. Section IV introduces a PII<sup>2</sup>RC and also gives a stability proof for the interconnection of an NI system a PII<sup>2</sup>RC. Section V introduces the HIGS-based PII<sup>2</sup>RC and shows that it can be applied in the stabilization of NI systems. In Section VI, we illustrate the main results in this paper that are given in Section III on a mass-spring system example. The paper is concluded in Section VII.

Notation: The notation in this paper is standard.  $\mathbb{R}$  denotes the field of real numbers.  $\mathbb{R}^{m \times n}$  denotes the space of real matrices of dimension  $m \times n$ .  $A^T$  denotes the transpose of a matrix  $A$ .  $A^{-T}$  denotes the transpose of the inverse of  $A$ ; that is,  $A^{-T} = (A^{-1})^T = (A^T)^{-1}$ .  $\lambda_{\max}(A)$  denotes the largest eigenvalue of a matrix  $A$  with real spectrum.  $\|\cdot\|$  denotes the standard Euclidean norm. For a real symmetric or complex Hermitian matrix  $P$ ,  $P > 0$  ( $P \geq 0$ ) denotes the positive (semi-)definiteness of a matrix  $P$  and  $P < 0$  ( $P \leq 0$ ) denotes the negative (semi-)definiteness of a matrix  $P$ . A function  $V : \mathbb{R}^n \rightarrow \mathbb{R}$  is said to be positive definite if  $V(0) = 0$  and  $V(x) > 0$  for all  $x \neq 0$ .

## II. PRELIMINARIES

### A. Negative imaginary systems

We consider systems of the form

$$\dot{x} = f(x, u), \quad (1a)$$

$$y = h(x), \quad (1b)$$

where  $x \in \mathbb{R}^n$ ,  $u, y \in \mathbb{R}^p$  are the state, input and output of the system, respectively. Here,  $f : \mathbb{R}^n \times \mathbb{R}^p \rightarrow \mathbb{R}^n$  is

a Lipschitz continuous function and  $h : \mathbb{R}^n \rightarrow \mathbb{R}^p$  is a continuously differentiable function. We assume  $f(0, 0) = 0$  and  $h(0) = 0$ .

*Definition 1 (NI systems):* [17], [18] A system of the form (1) is said to be a negative imaginary (NI) system if there exists a positive definite continuously differentiable storage function  $V : \mathbb{R}^n \rightarrow \mathbb{R}$  such that for any locally integrable input  $u$  and solution  $x$  to (1),

$$\dot{V}(x(t)) \leq u(t)^T \dot{y}(t), \quad \forall t \geq 0.$$

We provide the following conditions for a linear system to be NI. This condition is referred to as the NI lemma (see [37]).

*Lemma 1 (NI lemma):* [37] Let  $(A, B, C, D)$  be a minimal state-space realization of an  $p \times p$  real-rational proper transfer function matrix  $G(s)$  where  $A \in \mathbb{R}^{n \times n}$ ,  $B \in \mathbb{R}^{n \times p}$ ,  $C \in \mathbb{R}^{p \times n}$ ,  $D \in \mathbb{R}^{p \times p}$ . Then  $G(s)$  is NI if and only if:

1.  $\det A \neq 0$ ,  $D = D^T$ ;
2. There exists a matrix  $Y = Y^T > 0$ ,  $Y \in \mathbb{R}^{n \times n}$  such that

$$AY + YA^T \leq 0, \text{ and } B + AY C^T = 0. \quad (2)$$

### B. Integral resonant control

The implementation of an IRC is shown in Fig. 1. Given a SISO plant with a transfer function  $G(s)$ , we apply a direct feedthrough  $D$  and also an integral controller

$$C(s) = \frac{\Gamma}{s} \quad (3)$$

in positive feedback with  $G(s) + D$ . Here, we require the matrices  $\Gamma, D \in \mathbb{R}$  to satisfy  $D < 0$  and  $\Gamma > 0$ . The block diagram in Fig. 1 can be equivalently represented by the block diagram in Fig. 2, where  $K(s)$  is given as

$$K(s) = \frac{C(s)}{1 - C(s)D}. \quad (4)$$

Substituting (3) in (4), we obtain the transfer function of the IRC:

$$K(s) = \frac{\Gamma}{s - \Gamma D}. \quad (5)$$

An IRC is an SNI system, and can be used in the control of NI plants (see [1], [2], [33]).

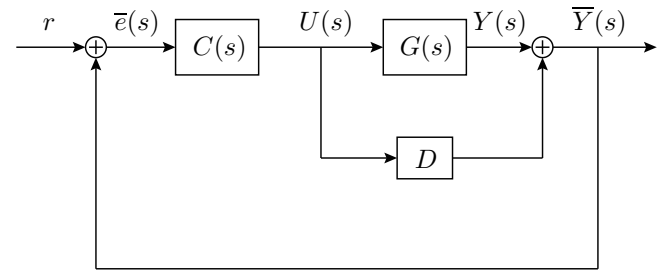


Fig. 1. Closed-loop interconnection of an integrator  $C(s) = \frac{\Gamma}{s}$  and  $G(s) + D$ .

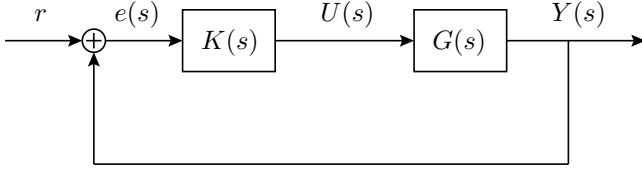


Fig. 2. Closed-loop interconnection of an IRC and a plant. This is equivalent to the closed-loop system in Fig. 1.

### C. Hybrid integrator-gain systems

A SISO hybrid integrator-gain system (HIGS)  $\mathcal{H}$  is represented by the following differential algebraic equations [20]:

$$\mathcal{H} : \begin{cases} \dot{x}_h = \omega_h e, & \text{if } (e, u, \dot{e}) \in \mathcal{F}_1 \\ x_h = k_h e, & \text{if } (e, u, \dot{e}) \in \mathcal{F}_2 \\ u = x_h, \end{cases} \quad (6)$$

where  $x_h, e, u \in \mathbb{R}$  denote the state, input, and output of the HIGS, respectively. Here,  $\dot{e}$  is the time derivative of the input  $e$ , which is assumed to be continuous and piecewise differentiable. Also,  $\omega_h \in [0, \infty)$  and  $k_h \in (0, \infty)$  represent the integrator frequency and gain value, respectively. These tunable parameters allow for desired control performance. The sets  $\mathcal{F}_1$  and  $\mathcal{F}_2 \in \mathbb{R}^3$  determine the HIGS modes of operation; i.e. the integrator and gain modes, respectively. The HIGS is designed to operate under the sector constraint  $(e, u, \dot{e}) \in \mathcal{F}$  (see [20], [38]) where

$$\mathcal{F} = \{(e, u, \dot{e}) \in \mathbb{R}^3 \mid eu \geq \frac{1}{k_h} u^2\}, \quad (7)$$

and  $\mathcal{F}_1$  and  $\mathcal{F}_2$  are defined as

$$\begin{aligned} \mathcal{F}_1 &= \mathcal{F} \setminus \mathcal{F}_2; \\ \mathcal{F}_2 &= \{(e, u, \dot{e}) \in \mathbb{R}^3 \mid u = k_h e \text{ and } \omega_h e^2 > k_h e \dot{e}\}. \end{aligned} \quad (8)$$

A HIGS of the form (6) is designed to primarily operate in the integrator mode unless the HIGS output  $u$  is on the boundary of the sector  $\mathcal{F}$ , and tends to exit the sector; i.e.  $(e, u, \dot{e}) \in \mathcal{F}_2$ . In this case, the HIGS is enforced to operate in the gain mode. At the time instants when switching happens, the state  $x_h$  still remains continuous, as can be seen from (6).

### III. HIGS-BASED IRC FOR NI SYSTEMS

In this section, we provide the system model of a HIGS-based IRC. Also, we show that a HIGS-based IRC has the NI property and can be applied in the control of an NI plant.

#### A. HIGS-based IRC

Consider the structure of an IRC as shown in Fig. 1. A HIGS-based IRC is constructed similarly but with the integrator  $C(s)$  in Fig. 1 replaced by a HIGS of the form (6). The implementation of a HIGS-based IRC is shown in Fig. 3.

We aim to derive the model of the HIGS-based IRC, which takes  $r + y$  as input and gives an output  $u$ , as shown in Fig. 4.

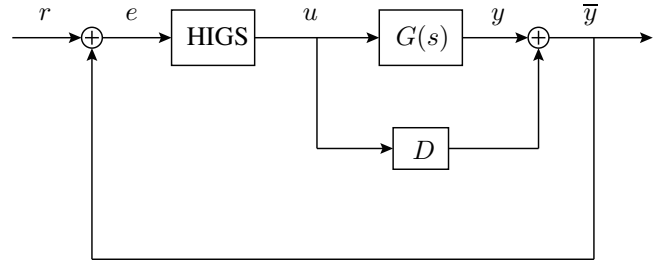


Fig. 3. Closed-loop interconnection of a HIGS  $\mathcal{H}$  and  $G(s) + D$ .

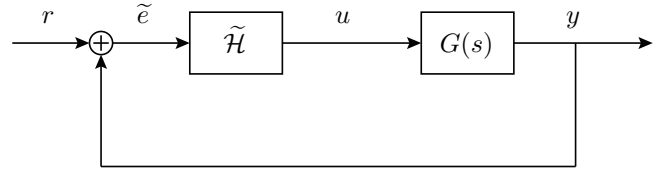


Fig. 4. Closed-loop interconnection of a HIGS-based IRC and a plant. It is equivalent to the closed-loop system in Fig. 3.

According to the settings in Fig. 3 and Fig. 4, we have that

$$\begin{aligned} e &= r + y + Du; \\ \tilde{e} &= r + y. \end{aligned} \quad (9)$$

Therefore, we have

$$e = \tilde{e} + Du = \tilde{e} + Dx_h, \quad (10)$$

where the second equality uses (6). When the HIGS is in the integrator mode, we have that

$$\dot{x}_h = \omega_h e = \omega_h Dx_h + \omega_h \tilde{e}.$$

When the HIGS is in the gain mode, we have that

$$x_h = k_h e = k_h Dx_h + k_h \tilde{e},$$

which implies

$$x_h = \frac{k_h}{1 - k_h D} \tilde{e}.$$

Also, we reformulate the sets  $\mathcal{F}$ ,  $\mathcal{F}_1$  and  $\mathcal{F}_2$  to pose conditions on  $(\tilde{e}, u, \dot{\tilde{e}})$  instead of  $(e, u, \dot{e})$ . Substituting (10) into (7) and (8), we have that

$$\tilde{\mathcal{F}} = \{(\tilde{e}, u, \dot{\tilde{e}}) \in \mathbb{R}^3 \mid \tilde{e}u \geq \frac{1 - k_h D}{k_h} u^2\},$$

$$\tilde{\mathcal{F}}_2 = \{(\tilde{e}, u, \dot{\tilde{e}}) \in \mathbb{R}^3 \mid u = \frac{k_h}{1 - k_h D} \tilde{e} \text{ and } \omega_h \tilde{e}^2 > k_h \tilde{e} \dot{\tilde{e}}\}.$$

To summarize, the system model of a HIGS-based IRC is given as follows:

$$\tilde{\mathcal{H}} : \begin{cases} \dot{x}_h = \omega_h Dx_h + \omega_h \tilde{e}, & \text{if } (\tilde{e}, u, \dot{\tilde{e}}) \in \tilde{\mathcal{F}}_1 \\ x_h = \tilde{e}, & \text{if } (\tilde{e}, u, \dot{\tilde{e}}) \in \tilde{\mathcal{F}}_2 \\ u = x_h, \end{cases} \quad (11)$$

where  $x_h, \tilde{e}, u \in \mathbb{R}$  are the state, input and output of the HIGS-based IRC, respectively. The variable  $\tilde{e}$  denotes the time derivative of the input  $\tilde{e}$  and is assumed to be continuous and piecewise differentiable. The constants  $\omega_h \geq 0$ ,  $D < 0$

and  $k_h > 0$  are the system parameters. Also, we denote the new gain value by

$$\tilde{\kappa} := \frac{k_h}{1 - k_h D} \quad (12)$$

since it will repeatedly occur in what follows. The HIGS-based IRC satisfies the sector constraint  $(\tilde{e}, u, \tilde{e}) \in \tilde{\mathcal{F}}$  where  $\tilde{\mathcal{F}}$ ,  $\tilde{\mathcal{F}}_1$  and  $\tilde{\mathcal{F}}_2$  are given as follows:

$$\tilde{\mathcal{F}} = \{(\tilde{e}, u, \tilde{e}) \in \mathbb{R}^3 \mid \tilde{e}u \geq \frac{1}{\tilde{\kappa}}u^2\}, \quad (13)$$

$$\tilde{\mathcal{F}}_1 = \tilde{\mathcal{F}} \setminus \tilde{\mathcal{F}}_2, \quad (14)$$

$$\tilde{\mathcal{F}}_2 = \{(\tilde{e}, u, \tilde{e}) \in \mathbb{R}^3 \mid u = \tilde{\kappa}\tilde{e} \text{ and } \omega_h \tilde{e}^2 > k_h \tilde{e}\tilde{e}\}. \quad (15)$$

### B. NI property of HIGS-based IRC

In this section, we show that a HIGS-based IRC of the form (11) is an NI system according to Definition 1.

*Theorem 1:* A HIGS-based IRC of the form (11) is an NI system with the storage function

$$V_h(x_h) = \frac{1}{2\tilde{\kappa}}x_h^2 \quad (16)$$

such that

$$\dot{V}_h(x_h) \leq \tilde{e}\dot{x}_h. \quad (17)$$

*Proof:* We have that  $\tilde{\kappa} > 0$  because in (12) we have  $k_h > 0$  and  $D < 0$ . Hence, the storage function  $V_h(x_h)$  in (16) is positive definite. We now show that (17) is satisfied in both integrator mode and gain mode. We have

$$\dot{V}_h(x_h) - \tilde{e}\dot{x}_h = \left(\frac{1}{\tilde{\kappa}}x_h - \tilde{e}\right)\dot{x}_h. \quad (18)$$

**Case 1.**  $(\tilde{e}, u, \tilde{e}) \in \tilde{\mathcal{F}}_1$ . In this case, we have  $\tilde{e}u \geq \frac{1}{\tilde{\kappa}}u^2$  according to (13) and (14). That is  $\tilde{e}x_h \geq \frac{1}{\tilde{\kappa}}x_h^2$  since  $u = x_h$ . According to the system dynamics in  $\tilde{\mathcal{F}}_1$  mode in (11), we have

$$\begin{aligned} \dot{V}_h(x_h) - \tilde{e}\dot{x}_h &= \left(\frac{1}{\tilde{\kappa}}x_h - \tilde{e}\right)(\omega_h D x_h + \omega_h \tilde{e}) \\ &= \frac{\omega_h}{\tilde{\kappa}}(x_h - \tilde{\kappa}\tilde{e})(D x_h + \tilde{e}). \end{aligned} \quad (19)$$

We discuss in the cases that  $x_h = 0$  and  $x_h \neq 0$ . If  $x_h = 0$ , then  $\dot{V}_h(x_h) - \tilde{e}\dot{x}_h = -\omega_h \tilde{e}^2 \leq 0$ . If  $x_h \neq 0$ , then sector constraint  $\tilde{e}x_h \geq \frac{1}{\tilde{\kappa}}x_h^2$  implies that  $\frac{\tilde{e}}{x_h} \geq \frac{1}{\tilde{\kappa}}$ . We can rewrite (19) as

$$\dot{V}_h(x_h) - \tilde{e}\dot{x}_h = \frac{\omega_h}{\tilde{\kappa}}x_h^2 \left(1 - \tilde{\kappa}\frac{\tilde{e}}{x_h}\right) \left(D + \frac{\tilde{e}}{x_h}\right). \quad (20)$$

The right-hand side of (20) is the product of a nonnegative quantity  $\frac{\omega_h}{\tilde{\kappa}}x_h^2$  and a function

$$\psi(a) = (1 - \tilde{\kappa}a)(D + a),$$

where  $a = \frac{\tilde{e}}{x_h} \geq \frac{1}{\tilde{\kappa}}$ . Letting  $\psi(a) = 0$ , we have that  $a = \frac{1}{\tilde{\kappa}}$  and  $a = -D$ . Note that  $\frac{1}{\tilde{\kappa}} = \frac{1}{k_h} - D > -D$ . The graph of the function  $\psi(a)$  is a parabola that opens downward and intersects with the horizontal axis at  $-D$  and  $\frac{1}{\tilde{\kappa}}$ . Therefore,  $\psi(a) \leq 0$  for all  $a \geq \frac{1}{\tilde{\kappa}}$ . This implies that  $\dot{V}_h(x_h) - \tilde{e}\dot{x}_h \leq 0$  also holds in the case  $x_h \neq 0$ .

**Case 2.**  $(\tilde{e}, u, \tilde{e}) \in \tilde{\mathcal{F}}_2$ . In this case, we have  $x_h = \tilde{\kappa}$

according to (15). Therefore, it follows from (18) that  $\dot{V}_h(x_h) - \tilde{e}\dot{x}_h = 0$ .

Therefore, the condition (17) is satisfied in both modes. Hence, HIGS-based IRC of the form (11) is an NI system.  $\blacksquare$

### C. Stability for the interconnection of an NI system and a HIGS-based IRC

Consider a SISO NI system with the transfer function  $G(s)$  and the minimal realization:

$$\dot{x} = Ax + Bu, \quad (21a)$$

$$y = Cx, \quad (21b)$$

where  $x \in \mathbb{R}^n$ ,  $u, y \in \mathbb{R}$  are the state, input and output of the system, respectively. Here,  $A \in \mathbb{R}^{n \times n}$ ,  $B \in \mathbb{R}^{n \times 1}$  and  $C \in \mathbb{R}^{1 \times n}$ . We show that for any NI plant of the form (21), there exists a HIGS-based IRC such that their closed-loop interconnection is asymptotically stable.

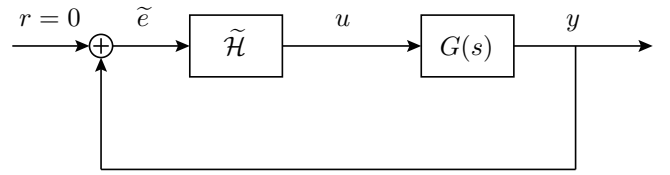


Fig. 5. Closed-loop interconnection of a HIGS-based IRC and a plant.

*Theorem 2:* Consider the SISO minimal linear NI system (21) with transfer function  $G(s)$ . There exists a HIGS-based IRC  $\tilde{\mathcal{H}}$  of the form (11) such that the closed-loop interconnection of the system (21) and the HIGS-based IRC  $\tilde{\mathcal{H}}$  as shown in Fig. 5 is asymptotically stable.

*Proof:* Since the system (21) is minimal and NI, then according to Lemma 1,  $\det A \neq 0$  and there exists a matrix  $Y = Y^T > 0$ ,  $Y \in \mathbb{R}^{n \times n}$  such that

$$AY + Y A^T \leq 0, \text{ and } B + AY C^T = 0. \quad (22)$$

We construct the candidate Lyapunov function of the closed-loop system as follows

$$W(x, x_h) = \frac{1}{2} \begin{bmatrix} x^T & x_h \end{bmatrix} \begin{bmatrix} Y^{-1} & -C^T \\ -C & \frac{1}{\tilde{\kappa}} \end{bmatrix} \begin{bmatrix} x \\ x_h \end{bmatrix}$$

Since  $Y > 0$ , then according to Schur complement theorem, the function  $W(x, x_h)$  is positive definite if and only if

$$\frac{1}{\tilde{\kappa}} - CYC^T > 0.$$

That is

$$\tilde{\kappa}G(0) < 1 \quad (23)$$

considering that  $G(0) = -CA^{-1}B = CA^{-1}AYC^T = CYC^T$ . We choose the parameters of the HIGS-based IRC to satisfy the condition (23). Also, since  $\tilde{\kappa} > 0$ , then  $W(x, x_h)$  is positive definite if and only if

$$Y^{-1} - \tilde{\kappa}C^T C > 0. \quad (24)$$

Therefore, (23) is satisfied if and only if (24) is satisfied. We apply Lyapunov stability theorem in the following. Taking the time derivative of the function  $W(x, x_h)$ , we have that

$$\begin{aligned}
\dot{W}(x, x_h) &= x^T Y^{-1} \dot{x} + \frac{1}{\kappa} x_h \dot{x}_h - \dot{x}_h C x - x_h C \dot{x} \\
&= (x^T Y^{-1} - x_h C) \dot{x} + \dot{x}_h \left( \frac{1}{\kappa} x_h - C x \right) \\
&= (x^T Y^{-1} - u C) \dot{x} + \dot{x}_h \left( \frac{1}{\kappa} x_h - \tilde{e} \right) \\
&= (x^T Y^{-1} + u B^T A^{-T} Y^{-1}) \dot{x} + \dot{x}_h \left( \frac{1}{\kappa} x_h - \tilde{e} \right) \\
&= (x^T A^T + u B^T) (A^{-T} Y^{-1}) \dot{x} + \dot{x}_h \left( \frac{1}{\kappa} x_h - \tilde{e} \right) \\
&= \dot{x}^T A^{-T} Y^{-1} \dot{x} + \dot{x}_h \left( \frac{1}{\kappa} x_h - \tilde{e} \right) \\
&= \frac{1}{2} \dot{x}^T (A^{-T} Y^{-1} + Y^{-1} A^{-1}) \dot{x} + \dot{x}_h \left( \frac{1}{\kappa} x_h - \tilde{e} \right), \tag{25}
\end{aligned}$$

where  $u = x_h$  and  $\tilde{e} = y = Cx$  are also used. The condition (22) implies that  $A^{-T} Y^{-1} + Y^{-1} A^{-1} \leq 0$ . Therefore,  $\frac{1}{2} \dot{x}^T (A^{-T} Y^{-1} + Y^{-1} A^{-1}) \dot{x} \leq 0$ . Also,  $\dot{x}_h (\frac{1}{\kappa} x_h - \tilde{e}) = \dot{V}_h(x_h) - \tilde{e} \dot{x}_h \leq 0$  as is shown in Theorem 1. Hence,  $\dot{W}(x, x_h) \leq 0$ . The closed-loop system is Lyapunov stable. We apply LaSalle's invariance principle in the following to show that the closed-loop system is indeed asymptotically stable. When  $\dot{W}(x, x_h)$  remains zero, we have both  $(A^{-T} Y^{-1} + Y^{-1} A^{-1}) \dot{x}$  and  $\dot{x}_h (\frac{1}{\kappa} x_h - \tilde{e})$  remaining zero. The condition  $\dot{x}_h (\frac{1}{\kappa} x_h - \tilde{e}) = 0$  implies that  $\dot{x}_h = 0$  or  $x_h = \kappa \tilde{e}$ . We show in the following that the condition  $\dot{x}_h = 0$  indeed also implies  $x_h = \kappa \tilde{e}$ . We only provide a proof for the case of  $\tilde{\mathcal{F}}_1$  mode since  $x_h = \kappa \tilde{e}$  is always true in the  $\tilde{\mathcal{F}}_2$  mode. According to the state equation in the  $\tilde{\mathcal{F}}_1$  mode given in (11), we have that  $\tilde{e} = -D x_h$ . Substituting this equation into the inequality in (13), we have that  $(-D - \frac{1}{\kappa}) x_h^2 \geq 0$ . Note that  $(-D - \frac{1}{\kappa}) = -\frac{1}{\kappa_h} < 0$ . Hence, in this case,  $x_h = 0$ . Therefore,  $\tilde{e} = -D x_h = 0$ . Thus,  $x_h = 0 = \kappa \tilde{e}$ . In the case that  $x_h \equiv \kappa \tilde{e}$ , we prove that the system cannot stay in the  $\tilde{\mathcal{F}}_1$  mode by contradiction. Suppose  $x_h \equiv \kappa \tilde{e}$  and  $\dot{x}_h = \omega_h D x_h + \omega_h \tilde{e}$ . Then,  $\tilde{e} = \omega_h D \kappa \tilde{e} + \omega_h \tilde{e}$ . That is  $\tilde{e} = \frac{\omega_h}{1 - \kappa_h D} \tilde{e}$ . This implies that both  $y$  and  $x_h$  diverge considering that  $\frac{\omega_h}{1 - \kappa_h D} > 0$ ,  $y = \tilde{e}$  and  $x_h = \kappa \tilde{e}$ . This contradicts the Lyapunov stability of the interconnection as shown above. Therefore, the HIGS-based IRC can only stay in the  $\tilde{\mathcal{F}}_2$  mode when  $x_h \equiv \kappa \tilde{e}$ . In this case, according to (15), we have

$$\omega_h \tilde{e}^2 > k_h \tilde{e} \dot{\tilde{e}}. \tag{26}$$

The condition (26) cannot be satisfied by satisfying  $\tilde{e} \dot{\tilde{e}} < 0$  over time because then  $\dot{V}_h(x_h) = \frac{1}{\kappa} x_h \dot{x}_h = \kappa \tilde{e} \dot{\tilde{e}} < 0$ . This implies that  $y = \tilde{e} = \frac{1}{\kappa} x_h$  converges to zero, which is not the case considered here. Also, in the case that (26) is satisfied with  $\tilde{e} = 0$  overtime, we have that  $\dot{y} = \dot{\tilde{e}} \equiv 0$ , which implies  $\dot{x} \equiv 0$  according to the observability of the system (21). The

quantity  $\dot{x}$  is given as follows

$$\begin{aligned}
\dot{x} &= Ax + Bu = Ax + Bx_h = Ax + B\kappa \tilde{e} = Ax + \kappa B y \\
&= Ax + \kappa BCx = (A + \kappa BC)x = (A - \kappa AY C^T C)x \\
&= AY(Y^{-1} - \kappa C^T C)x. \tag{27}
\end{aligned}$$

According to the nonsingularity of the matrices  $A$ ,  $Y$  and also (24),  $\dot{x} \neq 0$  for all  $x \neq 0$ . Therefore,  $\tilde{e} \equiv 0$  implies  $x = 0$  and  $x_h = 0$ . The system is already at the equilibrium. We have shown that (26) cannot be satisfied with  $\tilde{e} \dot{\tilde{e}} < 0$  overtime, and the case  $\tilde{e} = 0$  implies the system state is already at the equilibrium. Therefore, we only need to deal with the case that (26) is satisfied with  $\tilde{e} \dot{\tilde{e}} > 0$ . Since the trajectories of  $\tilde{e}$  and  $\dot{\tilde{e}}$  in the  $\tilde{\mathcal{F}}_2$  mode are independent of  $\omega_h$ , we can always choose sufficiently small  $\omega_h > 0$  such that  $\omega_h \tilde{e}^2 < k_h \tilde{e} \dot{\tilde{e}}$  in order to violate the condition (26). Therefore, the condition  $\dot{W}(x, x_h) \equiv 0$  can be violated by choosing suitable parameters. Then  $W(x, x_h)$  will keep decreasing until the system state reaches the origin. This implies that the interconnection in Fig. 5 is asymptotically stable. ■

#### IV. PROPORTIONAL-INTEGRAL-DOUBLE-INTEGRAL RESONANT CONTROL

In this section, we propose another variant of the IRC, where the integrator  $C(s)$  in Fig. 1 is replaced by a proportional-integral-double-integral (PII<sup>2</sup>) controller with the transfer function

$$\tilde{C}(s) = k_p + \frac{k_1}{s} + \frac{k_2}{s^2}. \tag{28}$$

Here,  $k_p, k_1, k_2 \in \mathbb{R}$  and we let  $k_p, k_1, k_2 > 0$ . Similar to the IRC, a PII<sup>2</sup> resonant controller (PII<sup>2</sup>RC) can be equivalently constructed as shown in Fig. 2, where the transfer function of the PII<sup>2</sup>RC is

$$\tilde{K}(s) = \frac{\tilde{C}(s)}{1 - \tilde{C}(s)D}. \tag{29}$$

Substituting (28) to (29), we obtain the transfer function of the PII<sup>2</sup>RC:

$$\tilde{K}(s) = \frac{k_p s^2 + k_1 s + k_2}{s^2 - k_p D s^2 - k_1 D s - k_2 D}. \tag{30}$$

**Lemma 2:** The PII<sup>2</sup>RC system with transfer function  $\tilde{K}(s)$  given in (30) is an SNI system.

*Proof:* Since  $k_p, k_1, k_2 > 0$  and  $D < 0$ , then the poles of  $\tilde{K}(s)$  satisfies  $\text{Re}[s] < 0$ . Also,

$$\begin{aligned}
j[\tilde{K}(j\omega) - \tilde{K}(-j\omega)] &= \frac{2k_1\omega^3}{((1 - k_p d)\omega^2 + k_2 d)^2 + (k_1 d\omega)^2} \\
&> 0, \tag{31}
\end{aligned}$$

for all  $\omega > 0$ . Therefore,  $\tilde{K}(s)$  is SNI. ■

**Theorem 3:** Consider the SISO minimal linear NI system (21) with transfer function  $G(s)$ . It can be stabilized using a PII<sup>2</sup>RC  $\tilde{K}(s)$  given in (30) satisfying  $D < -G(0)$ .

*Proof:* Since  $G(s)$  is NI with  $G(\infty) = 0$  and  $\tilde{K}(s)$  is SNI, then the interconnection of  $G(s)$  and  $\tilde{K}(s)$  is asymptotically stable if and only if  $G(0)\tilde{K}(0) < 1$ . According to

(30),  $K(0) = -\frac{1}{D}$ . Therefore, stability is achieved if and only if  $G(0)(-\frac{1}{D}) < 1$ . That is,  $D < -G(0)$ . Note that here  $G(0) = -CA^{-1}B = CYC^T \geq 0$ , according to Lemma 1. ■

## V. HIGS-BASED PII<sup>2</sup>RC

Motivated by the PII<sup>2</sup>RC proposed in Section IV, we consider a HIGS-based PII<sup>2</sup>RC in this section. To be specific, we consider replacing the single integrator  $k_1/s$  in the PII<sup>2</sup>RC by a single HIGS of the form (6). Also, we replace the double integrator  $k_2/s^2$  by two serial cascaded HIGS, both of the form (6).

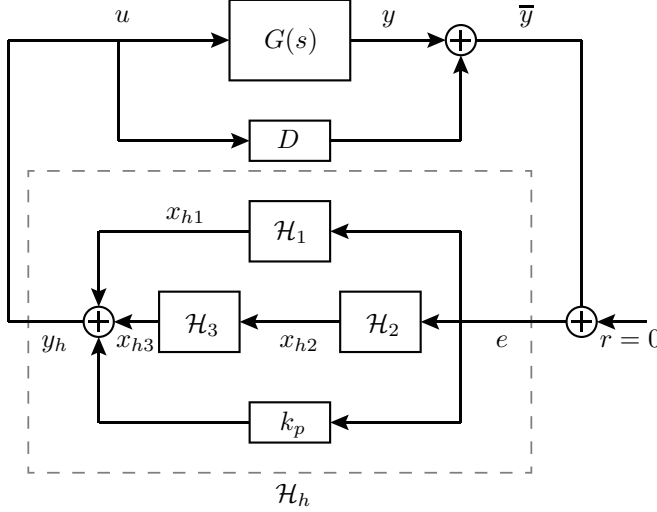


Fig. 6. Closed-loop interconnection of a HIGS-based PII<sup>2</sup> controller  $\mathcal{H}_h$  and  $G(s) + D$ . The system  $\mathcal{H}_h$  as shown in the dotted line box with input  $e$  and output  $y_h$  is the parallel cascade of a single HIGS  $\mathcal{H}_1$ , the serial cascade of two HIGS  $\mathcal{H}_2$  and  $\mathcal{H}_3$ , and also a gain  $k_p$ .

The HIGS  $\mathcal{H}_1$ ,  $\mathcal{H}_2$  and  $\mathcal{H}_3$  are of the form (6), with different parameters. We provide the system models of  $\mathcal{H}_1$ ,  $\mathcal{H}_2$  and  $\mathcal{H}_3$  again in the following to distinguish different parameters in these three HIGS:

$$\mathcal{H}_i : \begin{cases} \dot{x}_{hi} = \omega_{hi}e_i, & \text{if } (e_i, x_{hi}, \dot{e}_i) \in \mathcal{F}_{i1} \\ x_{hi} = k_{hi}e_i, & \text{if } (e_i, x_{hi}, \dot{e}_i) \in \mathcal{F}_{i2} \end{cases} \quad (32)$$

where  $e_i \in \mathbb{R}$  is the input,  $x_{hi} \in \mathbb{R}$  is the state and also the output of the HIGS  $\mathcal{H}_i$  ( $i = 1, 2, 3$ ), respectively. Here,  $\dot{e}_i$  is the time derivative of the input  $e_i$ , which is assumed to be continuous and piecewise differentiable. The parameters  $\omega_{hi} \in [0, \infty)$  and  $k_{hi} \in (0, \infty)$  represent the integrator frequency and gain value of the HIGS  $\mathcal{H}_i$ , respectively. Also, we have

$$\mathcal{F}_i = \{(e_i, x_{hi}, \dot{e}_i) \in \mathbb{R}^3 \mid e_i x_{hi} \geq \frac{1}{k_{hi}} x_{hi}^2\}, \quad (33)$$

$$\mathcal{F}_{i1} = \mathcal{F}_i \setminus \mathcal{F}_{i2}; \quad (34)$$

$$\mathcal{F}_{i2} = \{(e_i, x_{hi}, \dot{e}_i) \in \mathbb{R}^3 \mid x_{hi} = k_{hi}e_i \text{ and } \omega_{hi}e_i^2 > k_{hi}e_i\dot{e}_i\}. \quad (35)$$

According to the setting of the system  $\mathcal{H}_h$  in Fig. 6, we have that

$$e_1 = e_2 = e; \text{ and } e_3 = x_{h2}.$$

The integrator frequency  $\omega_{h1}$  of the HIGS  $\mathcal{H}_1$  corresponds to the parameter  $k_1$  of the PII<sup>2</sup> controller  $\tilde{C}(s)$  given in (28). Also, the product of the integrator frequencies  $\omega_{h2}$  and  $\omega_{h3}$  corresponds to the parameter  $k_2$  in (28).

We prove in the following that the closed-loop interconnection shown in Fig. 6 is asymptotically stable. First, we provide some preliminary results on the nonlinear NI property of a single HIGS and two cascaded HIGS; see also [28]. Note that the notation used in the present paper is different from that in [28].

*Lemma 3:* (see [27], [28]) A HIGS  $\mathcal{H}_1$  of the form (32) is a nonlinear NI system from the input  $e_1$  to the output  $x_{h1}$  with the storage function

$$V_1(x_{h1}) = \frac{1}{2k_{h1}} x_{h1}^2$$

satisfying

$$\dot{V}(x_{h1}) \leq e_1 \dot{x}_{h1}. \quad (36)$$

Also, if  $\dot{V}(x_{h1}) = e_1 \dot{x}_{h1}$  then for all  $t \in [t_a, t_b]$  we have that  $x_{h1} = k_{h1}e_1$ .

*Lemma 4:* (see also [28]) Consider a HIGS  $\mathcal{H}_1$  of the form (32). If  $\dot{V}(x_{h1}) = e_1 \dot{x}_{h1}$ , then  $x_{h1} = k_{h1}e_1$ .

*Proof:* This lemma is a special single channel case of Lemma 4 in [28]. ■

For the cascade of the HIGS  $mc\mathcal{H}_2$  and  $\mathcal{H}_3$ , we assume that

$$k_{h2} = k_{h3}, \text{ and } \omega_{h2} < \omega_{h3}. \quad (37)$$

This assumption simplifies the proof of Lemma 5, which is further used Theorem 1. As Theorem 4 shows the existence of a stabilizing HIGS-based PII<sup>2</sup>RC for an NI plant. Therefore, (37) is not a necessary condition for choosing a stabilizing HIGS-based PII<sup>2</sup>RC.

*Lemma 5:* (see [28]) Consider two HIGS  $\mathcal{H}_2$  and  $\mathcal{H}_3$  of the form (32) and satisfy (37). Then the serial cascade of  $\mathcal{H}_2$  and  $\mathcal{H}_3$  as shown in Fig. 7 is a nonlinear NI system from the input  $e_2$  to the output  $x_{h3}$  with the storage function

$$V_2(x_{h2}, x_{h3}) = \frac{1}{2} x_{h2}^2 \quad (38)$$

satisfying

$$\dot{V}(x_{h2}, x_{h3}) \leq e_2 \dot{x}_{h3}. \quad (39)$$

Moreover, if  $\dot{V}(x_{h2}, x_{h3}) = e_2 \dot{x}_{h3}$  over a time interval  $[t_a, t_b]$ , where  $t_a < t_b$ , then for all  $t \in [t_a, t_b]$  we have that  $x_{h2} = k_{h2}e_2$  and  $x_{h3} = k_{h3}x_{h2} = k_{h2}^2 e_2$ .

*Proof:* The proof follows directly from Theorem 5 in [28], with (37) assumed. The parameter  $a$  in Theorem 5 in [28] is allowed to take the value  $a = \frac{k_{h3}}{2k_{h2}} = \frac{1}{2}$ , which results the storage function  $V_2(x_{h2}, x_{h3})$  in (38) to be positive semidefinite instead of positive definite. Regarding the analysis of the case where  $\dot{V}(x_{h2}, x_{h3}) = e_2 \dot{x}_{h3}$  over a finite time interval, the proof of Theorem 5 in [28] still remains valid under the assumptions (37) and  $a = \frac{1}{2}$ , with slight modifications. ■

*Theorem 4:* Consider the SISO minimal linear NI system (21) with transfer function  $G(s)$ . Also, consider a HIGS-based PII<sup>2</sup> controller  $\mathcal{H}_h$  applied in positive feedback with



Fig. 7. The serial cascade of two HIGS  $\mathcal{H}_2$  and  $\mathcal{H}_3$

$G(s) + D$ , as shown in Fig. 6, where  $D < 0$  is a scalar. Here,  $\mathcal{H}_h$  is the parallel cascade of the HIGS  $\mathcal{H}_1$ , the serial cascade of two HIGS  $\mathcal{H}_2$  and  $\mathcal{H}_3$ , and also a gain  $k_p > 0$ . Each HIGS is of the form (32), where (37) is also assumed. Then there exists a set of parameters  $\{D, k_p, \omega_{h1}, \omega_{h2}, k_{h1}, k_{h2}\}$  such that the closed-loop system shown in Fig. 6 is asymptotically stable.

*Proof:* According to Fig. 6, we have that

$$\begin{aligned} e &= Cx + Du = Cx + D(x_{h1} + x_{h3} + k_p e) \\ \Rightarrow e &= \gamma Cx + \gamma D(x_{h1} + x_{h3}), \end{aligned} \quad (40)$$

where

$$\gamma = \frac{1}{1 - Dk_p} > 0. \quad (41)$$

Also, we have that

$$\begin{aligned} u &= x_{h1} + x_{h3} + k_p e \\ &= k_p \gamma Cx + \gamma(x_{h1} + x_{h3}) \end{aligned} \quad (42)$$

We apply Lyapunov's direct method using the candidate Lyapunov function

$$W(x, x_{h1}, x_{h2}, x_{h3}) = \frac{1}{2} \begin{bmatrix} x^T & x_{h1} & x_{h2} & x_{h3} \end{bmatrix} M \begin{bmatrix} x \\ x_{h1} \\ x_{h2} \\ x_{h3} \end{bmatrix} \quad (43)$$

where

$$M = \begin{bmatrix} Y^{-1} - k_p \gamma C^T C & -\gamma C^T & 0 & -\gamma C^T \\ -\gamma C & \frac{1}{k_{h1}} - D\gamma & 0 & -D\gamma \\ 0 & 0 & 1 & 0 \\ -\gamma C & -D\gamma & 0 & -D\gamma \end{bmatrix}.$$

First, we show the positive definiteness of the function  $W(x, x_{h1}, x_{h2}, x_{h3})$  by showing  $M > 0$ . Observing the third block row and block column of  $M$ , we have  $M > 0$  if and only if

$$\widetilde{M} = \begin{bmatrix} Y^{-1} - k_p \gamma C^T C & -\gamma C^T & -\gamma C^T \\ -\gamma C & \frac{1}{k_{h1}} - D\gamma & -D\gamma \\ -\gamma C & -D\gamma & -D\gamma \end{bmatrix} > 0.$$

Since  $k_p > 0$  and  $D < 0$ , we have that  $\gamma > 0$ . Therefore,  $\widetilde{M} > 0$  if and only if

$$\widehat{M} = \frac{1}{\gamma} \widetilde{M} = \begin{bmatrix} \frac{1}{\gamma} Y^{-1} - k_p C^T C & -C^T & -C^T \\ -C & \frac{1}{k_{h1} \gamma} - D & -D \\ -C & -D & -D \end{bmatrix} > 0 \quad (44)$$

We apply Schur complement theorem in the following. Observing that the 3, 3 block  $\widehat{M}_{33} = -D > 0$ , then  $\widehat{M} > 0$

if and only if

$$\begin{aligned} \overline{M} &= \widehat{M} / \widehat{M}_{33} \\ &= \begin{bmatrix} \frac{1}{\gamma} Y^{-1} - k_p C^T C & -C^T \\ -C & \frac{1}{k_{h1} \gamma} - D \end{bmatrix} + \frac{1}{D} \begin{bmatrix} C^T \\ D \end{bmatrix} \begin{bmatrix} C & D \end{bmatrix} \\ &= \begin{bmatrix} \frac{1}{\gamma} Y^{-1} - (k_p - \frac{1}{D}) C^T C & 0 \\ 0 & \frac{1}{k_{h1} \gamma} \end{bmatrix} \end{aligned} \quad (45)$$

Since  $\frac{1}{k_{h1} \gamma} > 0$ , then we have  $\overline{M} > 0$  if and only if

$$\frac{1}{\gamma} Y^{-1} - (k_p - \frac{1}{D}) C^T C > 0 \quad (46)$$

Substituting (41) into (46), we have that (46) holds if and only if

$$Y^{-1} + \frac{1}{D} C^T C > 0 \quad (47)$$

Using Schur complement theorem, (47) is equivalent to the positive definiteness of the matrix

$$Q = \begin{bmatrix} Y^{-1} & C^T \\ C & -D \end{bmatrix} \quad (48)$$

Also, considering that  $Y > 0$ , we have  $Q > 0$  if and only if

$$-D - CYC^T > 0. \quad (49)$$

Considering that  $G(0) = -CA^{-1}B = CYC^T$  according to (2), the condition (49) can be expressed as

$$D < -G(0). \quad (50)$$

Therefore, the function  $W(x, x_{h1}, x_{h2}, x_{h3})$  given in (43) is positive definite if and only if (50) is satisfied. Taking the time derivative of  $W(x, x_{h1}, x_{h2}, x_{h3})$ , we have

$$\begin{aligned} \dot{W}(x, x_{h1}, x_{h2}, x_{h3}) &= x^T Y^{-1} \dot{x} + \frac{1}{k_{h1}} x_{h1} \dot{x}_{h1} + x_{h2} \dot{x}_{h2} - \gamma(\dot{x}_{h1} + \dot{x}_{h3}) Cx \\ &\quad - \gamma(x_{h1} + x_{h3}) C \dot{x} - \gamma D(x_{h1} + x_{h3})(\dot{x}_{h1} + \dot{x}_{h3}) \\ &\quad - k_p \gamma x^T C^T C \dot{x} \\ &= [x^T Y^{-1} - (\gamma(x_{h1} + x_{h3}) - k_p \gamma x^T C^T)] C \dot{x} \\ &\quad + \left[ \frac{1}{k_{h1}} x_{h1} \dot{x}_{h1} - (\gamma Cx + \gamma D(x_{h1} + x_{h3})) \dot{x}_{h1} \right] \\ &\quad + [x_{h2} \dot{x}_{h2} - (\gamma Cx + \gamma D(x_{h1} + x_{h3})) \dot{x}_{h3}] \\ &= (x^T Y^{-1} - uC) \dot{x} + (\dot{V}_1(x_{h1}) - e \dot{x}_{h1}) \\ &\quad + (\dot{V}_2(x_{h2}, x_{h3}) - e \dot{x}_{h3}). \end{aligned} \quad (51)$$

We have that

$$\begin{aligned} (x^T Y^{-1} - uC) \dot{x} &= (x^T A^T A^{-T} Y^{-1} + uB^T A^{-T} Y^{-1}) \dot{x} \\ &= (x^T A^T + uB^T) A^{-T} Y^{-1} \dot{x} \\ &= \dot{x}^T (A^{-T} Y^{-1}) \dot{x} \\ &= \frac{1}{2} \dot{x}^T (A^{-T} Y^{-1} + Y^{-1} A^{-1}) \dot{x} \\ &\leq 0. \end{aligned} \quad (52)$$

Also, we have that  $\dot{V}_1(x_{h1}) - e \dot{x}_{h1} \leq 0$  and  $\dot{V}_2(x_{h2}, x_{h3}) - e \dot{x}_{h3} \leq 0$  according to the NI property of the  $\mathcal{H}_1$  and

the cascade of  $\mathcal{H}_2$  and  $\mathcal{H}_3$ , as shown in Lemmas 3 and 5. Therefore,  $\dot{W}(x, x_{h1}, x_{h2}, x_{h3}) \leq 0$ , which implies that the closed-loop interconnection in Fig. 6 is Lyapunov stable. We apply LaSalle's invariance principle in the following to show asymptotic stability. In the case that  $\dot{W}(x, x_{h1}, x_{h2}, x_{h3})$  remains zero, we have that  $\dot{x}^T(A^{-T}Y^{-1} + Y^{-1}A^{-1})\dot{x} \equiv 0$ ,  $\dot{V}_1(x_{h1}) - e\dot{x}_{h1} \equiv 0$  and  $\dot{V}_2(x_{h2}, x_{h3}) - e\dot{x}_{h3} \equiv 0$ . According to Lemma 4,  $\dot{V}_1(x_{h1}) - e\dot{x}_{h1} \equiv 0$  implies

$$x_{h1} \equiv k_{h1}e. \quad (53)$$

Also, according to Lemma 5,  $\dot{V}_2(x_{h2}, x_{h3}) - e\dot{x}_{h3} \equiv 0$  implies

$$x_{h2} \equiv k_{h2}e, \quad (54)$$

$$x_{h3} \equiv k_{h2}^2e. \quad (55)$$

We show that the HIGS  $\mathcal{H}_1$ ,  $\mathcal{H}_2$  and  $\mathcal{H}_3$  cannot stay in the integrator mode  $\mathcal{F}_{i1}$  by contradiction. According to (32), if  $(e_i, x_{hi}, \dot{e}_i) \in \mathcal{F}_{i1}$ , then  $\dot{x}_{hi} = \omega_{hi}e_i$ . Since  $x_{hi} = k_{hi}e_i$ , then we have  $k_{hi}\dot{e}_i = \omega_{hi}e_i$ . That is,

$$\dot{e}_i = \frac{\omega_{hi}}{k_{hi}}e_i,$$

which implies that  $e_i$  diverges and so is  $x_{hi}$ . This contradicts the Lyapunov stability of the interconnection that is proved above. Therefore, the HIGS  $\mathcal{H}_1$ ,  $\mathcal{H}_2$  and  $\mathcal{H}_3$  all stay in the gain mode  $\mathcal{F}_{i2}$ . In this case, according to (35), we have that  $\omega_{hi}e_i^2 > k_{hi}e_i\dot{e}_i$ . That is

$$\begin{aligned} \omega_{h1}e^2 &> k_{h1}e\dot{e}; \\ \omega_{h2}e^2 &> k_{h2}e\dot{e}; \\ \omega_{h2}x_{h2}^2 &> k_{h2}x_{h2}\dot{x}_{h2} \implies \omega_{h2}e^2 > k_{h2}e\dot{e}, \end{aligned}$$

for  $\mathcal{H}_1$ ,  $\mathcal{H}_2$  and  $\mathcal{H}_3$ , respectively. Hence, we have

$$\rho e^2 > e\dot{e}, \quad (56)$$

where  $\rho = \min\{\frac{\omega_{h1}}{k_{h1}}, \frac{\omega_{h2}}{k_{h2}}\}$ . We show in the following that the condition (56) can be satisfied over time by satisfying  $e\dot{e} < 0$ . In this case that  $e\dot{e} < 0$ , the HIGS input  $e$  converges. This implies that  $x_{h1}$ ,  $x_{h2}$  and  $x_{h3}$  all converge to zero. Also, according to (40) and (42),  $y$  and  $u$  also converge. This is not the case of  $\dot{W}(x, x_{h1}, x_{h2}, x_{h3}) \equiv 0$  that is considered here. Also, we can avoid the case that (56) is satisfied by satisfying  $\dot{e} \equiv 0$  overtime. When  $e$  is a constant, the HIGS states  $x_{h1}$ ,  $x_{h2}$  and  $x_{h3}$  are all constants, according to (53), (54) and (55). Also, according to (40) and (42), we have that  $y = Cx$  is a constant and also  $u$  is a constant. Since the system (21) is observable, we have that  $\dot{x} = 0$  and the system (21) is in a steady state. Denote the constant values of  $u$  and  $e$  by  $\bar{u}$  and  $\bar{e}$ , respectively, we have that

$$\bar{u} = (k_{h1} + k_{h2}^2 + k_p)\bar{e},$$

according to the system setting in Fig. 6. Also, we have that

$$\bar{e} = (G(0) + D)\bar{u}.$$

Therefore, by choosing suitable parameters  $k_{h1}$ ,  $k_{h2}$ , and  $k_p$  such that

$$k_{h1} + k_{h2}^2 + k_p \neq \frac{1}{G(0) + D},$$

we can avoid the case that  $\dot{e} \equiv 0$ . Hence,  $e\dot{e} > 0$  will be satisfied eventually. In this case, since the trajectories of  $e$  and  $\dot{e}$  are independent of  $\omega_{h1}$  and  $\omega_{h2}$  when all of the HIGS are in the gain mode  $\mathcal{F}_{i2}$ , then we can always choose  $\omega_{h1}$  or  $\omega_{h2}$  to be sufficiently small such that  $\rho e^2 < e\dot{e}$ . Therefore,  $\dot{W}(x, x_{h1}, x_{h2}, x_{h3})$  cannot remain zero over time and  $\dot{W}(x, x_{h1}, x_{h2}, x_{h3})$  will keep decreasing until  $\dot{W}(x, x_{h1}, x_{h2}, x_{h3}) = 0$ . This implies that the interconnection in Fig. 6 is asymptotically stable. ■

## VI. EXAMPLE

In this section, we apply the proposed HIGS-based IRC to stabilize a mass-spring system. As is shown in Fig. 8, the mass of the cart is  $m = 1kg$  and the spring constant is  $k = 1N/m$ . The state-space model of the system is given as follows:

$$\begin{aligned} \dot{x} &= \begin{bmatrix} 0 & 1 \\ -1 & 0 \end{bmatrix} x + \begin{bmatrix} 0 \\ 1 \end{bmatrix} u; \\ y &= \begin{bmatrix} 1 & 0 \end{bmatrix} x, \end{aligned} \quad (57)$$

where  $x = \begin{bmatrix} x_1 \\ x_2 \end{bmatrix}$  is the system state with  $x_1$  and  $x_2$  being its displacement and velocity, respectively. Also,  $u$  is an external force input and we measure the system displacement as its output  $y$ . The system (57) has a transfer function  $G(s) =$

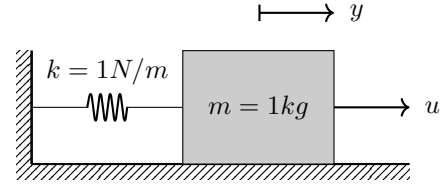


Fig. 8. A mass-spring system with mass  $m = 1kg$  and spring constant  $k = 1N/m$ .

$\frac{1}{s^2+1}$ . We construct a HIGS-based IRC of the form (11) with

$$\omega_h = 0.5, \quad k_h = 20, \quad D = -1. \quad (58)$$

Using (12), we have that  $\tilde{\kappa} = \frac{5}{6}$ . Such a  $\tilde{\kappa}$  satisfies the condition  $\tilde{\kappa}G(0) < 1$ . We set the initial state of the system (57) be  $x_1(0) = 3, x_2(0) = 1$ . The initial state of the HIGS-based IRC is set to be zero. We can see from Fig. 9 that the states of the system (57) converge to the origin under the effect of the HIGS-based IRC.

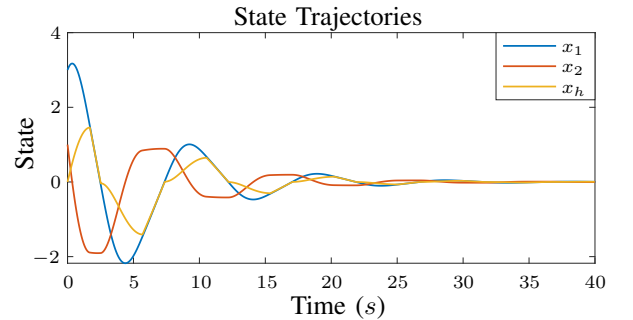


Fig. 9. State trajectories for the feedback interconnection of the system (57) and a HIGS-based IRC with parameters (58).



## VII. CONCLUSION

In this paper, we introduce a HIGS-based IRC to provide a control approach for an NI system, with the advantages of both HIGS and IRC utilized. A HIGS-based IRC is achieved by replacing the integrator in an IRC by a HIGS element. We show that a HIGS-based IRC is an NI system and can stabilize an NI plant when applied in positive feedback. Also, we propose a  $\text{PII}^2\text{RC}$  and a HIGS-based  $\text{PII}^2\text{RC}$  for the control of NI systems. We show that both a  $\text{PII}^2\text{RC}$  and a HIGS-based  $\text{PII}^2\text{RC}$  can provide asymptotic stabilization for an NI system. An illustrative example is also provided.

## REFERENCES

- [1] A. Lanzon and I. R. Petersen, "Stability robustness of a feedback interconnection of systems with negative imaginary frequency response," *IEEE Transactions on Automatic Control*, vol. 53, no. 4, pp. 1042–1046, 2008.
- [2] I. R. Petersen and A. Lanzon, "Feedback control of negative-imaginary systems," *IEEE Control Systems Magazine*, vol. 30, no. 5, pp. 54–72, 2010.
- [3] A. Preumont, *Vibration control of active structures: an introduction*. Springer, 2018, vol. 246.
- [4] D. Halim and S. O. R. Moheimani, "Spatial resonant control of flexible structures-application to a piezoelectric laminate beam," *IEEE Transactions on Control Systems Technology*, vol. 9, no. 1, pp. 37–53, 2001.
- [5] H. Pota, S. O. R. Moheimani, and M. Smith, "Resonant controllers for smart structures," *Smart Materials and Structures*, vol. 11, no. 1, p. 1, 2002.
- [6] B. Brogliato, R. Lozano, B. Maschke, and O. Ekeland, *Dissipative systems analysis and control: theory and applications*. Springer, London, 2007, vol. 2.
- [7] K. Shi, I. R. Petersen, and I. G. Vladimirov, "Necessary and sufficient conditions for state feedback equivalence to negative imaginary systems," *IEEE Transactions on Automatic Control (Early Access)*, 2024.
- [8] A. Lanzon and H.-J. Chen, "Feedback stability of negative imaginary systems," *IEEE Transactions on Automatic Control*, vol. 62, no. 11, pp. 5620–5633, 2017.
- [9] M. A. Mabrok, A. G. Kallapur, I. R. Petersen, and A. Lanzon, "Spectral conditions for negative imaginary systems with applications to nanopositioning," *IEEE/ASME Transactions on Mechatronics*, vol. 19, no. 3, pp. 895–903, 2013.
- [10] S. K. Das, H. R. Pota, and I. R. Petersen, "A MIMO double resonant controller design for nanopositioners," *IEEE Transactions on Nanotechnology*, vol. 14, no. 2, pp. 224–237, 2014.
- [11] —, "Resonant controller design for a piezoelectric tube scanner: A mixed negative-imaginary and small-gain approach," *IEEE Transactions on Control Systems Technology*, vol. 22, no. 5, pp. 1899–1906, 2014.
- [12] —, "Multivariable negative-imaginary controller design for damping and cross coupling reduction of nanopositioners: a reference model matching approach," *IEEE/ASME Transactions on Mechatronics*, vol. 20, no. 6, pp. 3123–3134, 2015.
- [13] C. Cai and G. Hagen, "Stability analysis for a string of coupled stable subsystems with negative imaginary frequency response," *IEEE Transactions on Automatic Control*, vol. 55, no. 8, pp. 1958–1963, 2010.
- [14] M. A. Rahman, A. Al Mamun, K. Yao, and S. K. Das, "Design and implementation of feedback resonance compensator in hard disk drive servo system: A mixed passivity, negative-imaginary and small-gain approach in discrete time," *Journal of Control, Automation and Electrical Systems*, vol. 26, no. 4, pp. 390–402, 2015.
- [15] B. Bhikkaji, S. O. R. Moheimani, and I. R. Petersen, "A negative imaginary approach to modeling and control of a collocated structure," *IEEE/ASME Transactions on Mechatronics*, vol. 17, no. 4, pp. 717–727, 2011.
- [16] Y. Chen, K. Shi, I. R. Petersen, and E. L. Ratnam, "A nonlinear negative imaginary systems framework with actuator saturation for control of electrical power systems," *To appear in 2024 European Control Conference*, 2023.
- [17] A. G. Ghallab, M. A. Mabrok, and I. R. Petersen, "Extending negative imaginary systems theory to nonlinear systems," in *2018 IEEE Conference on Decision and Control (CDC)*. IEEE, 2018, pp. 2348–2353.
- [18] K. Shi, I. G. Vladimirov, and I. R. Petersen, "Robust output feedback consensus for networked identical nonlinear negative-imaginary systems," *IFAC-PapersOnLine*, vol. 54, no. 9, pp. 239–244, 2021.
- [19] K. Shi, I. R. Petersen, and I. G. Vladimirov, "Output feedback consensus for networked heterogeneous nonlinear negative-imaginary systems with free-body motion," *IEEE Transactions on Automatic Control*, vol. 68, no. 9, pp. 5536–5543, 2023.
- [20] D. A. Deenen, M. F. Heertjes, W. Heemels, and H. Nijmeijer, "Hybrid integrator design for enhanced tracking in motion control," in *2017 American Control Conference (ACC)*. IEEE, 2017, pp. 2863–2868.
- [21] R. H. Middleton, "Trade-offs in linear control system design," *Automatica*, vol. 27, no. 2, pp. 281–292, 1991.
- [22] S. Van den Eijnden, M. F. Heertjes, W. Heemels, and H. Nijmeijer, "Hybrid integrator-gain systems: A remedy for overshoot limitations in linear control?" *IEEE Control Systems Letters*, vol. 4, no. 4, pp. 1042–1047, 2020.
- [23] D. Van Dinther, B. Sharif, S. Van den Eijnden, H. Nijmeijer, M. F. Heertjes, and W. Heemels, "Overcoming performance limitations of linear control with hybrid integrator-gain systems," *IFAC-PapersOnLine*, vol. 54, no. 5, pp. 289–294, 2021.
- [24] M. Heertjes, S. van Den Eijnden, and B. Sharif, "An overview on hybrid integrator-gain systems with applications to wafer scanners," in *2023 IEEE International Conference on Mechatronics (ICM)*. IEEE, 2023, pp. 1–8.
- [25] D. A. Deenen, B. Sharif, S. van den Eijnden, H. Nijmeijer, M. Heemels, and M. Heertjes, "Projection-based integrators for improved motion control: Formalization, well-posedness and stability of hybrid integrator-gain systems," *Automatica*, vol. 133, p. 109830, 2021.
- [26] S. van den Eijnden, M. Heertjes, H. Nijmeijer, and W. Heemels, "A small-gain approach to incremental input-to-state stability analysis of hybrid integrator-gain systems," *IEEE Control Systems Letters*, 2023.
- [27] K. Shi, N. Nikoienjad, I. R. Petersen, and S. O. R. Moheimani, "A negative imaginary approach to hybrid integrator-gain system control," in *2022 IEEE 61st Conference on Decision and Control (CDC)*. IEEE, 2022, pp. 1968–1973.
- [28] —, "Negative imaginary control using hybrid integrator-gain systems: Application to MEMS nanopositioner," *IEEE Transactions on Control Systems Technology (Early Access)*, 2023.
- [29] K. Shi, I. R. Petersen, and I. G. Vladimirov, "Nonlinear negative imaginary systems with switching," *IFAC-PapersOnLine*, vol. 56, no. 2, pp. 3936–3941, 2023.
- [30] —, "Discrete-time negative imaginary systems from ZOH sampling," *To appear in the proceedings of the 26th International Symposium on Mathematical Theory of Networks and Systems (MTNS)*, arXiv preprint:2312.05419, 2024.
- [31] K. Shi and I. R. Petersen, "Digital control of negative imaginary systems: a discrete-time hybrid integrator-gain system approach," *To appear in 2024 European Control Conference*, 2024.
- [32] S. S. Aphale, A. J. Fleming, and S. R. Moheimani, "Integral resonant control of collocated smart structures," *Smart materials and structures*, vol. 16, no. 2, p. 439, 2007.
- [33] B. Bhikkaji, S. R. Moheimani, and I. R. Petersen, "Multivariable integral control of resonant structures," in *2008 47th IEEE Conference on Decision and Control*. IEEE, 2008, pp. 3743–3748.
- [34] Y. Yue and Z. Song, "An integral resonant control scheme for a laser beam stabilization system," in *2015 IEEE International Conference on Information and Automation*. IEEE, 2015, pp. 2221–2226.
- [35] B. Bhikkaji and S. R. Moheimani, "Integral resonant control of a piezoelectric tube actuator for fast nanoscale positioning," *IEEE/ASME Transactions on mechatronics*, vol. 13, no. 5, pp. 530–537, 2008.
- [36] D. Russell and S. S. Aphale, "Evaluating the performance of robust controllers for a nanopositioning platform under loading," *IFAC-PapersOnLine*, vol. 50, no. 1, pp. 10 895–10 900, 2017.
- [37] J. Xiong, I. R. Petersen, and A. Lanzon, "A negative imaginary lemma and the stability of interconnections of linear negative imaginary systems," *IEEE Transactions on Automatic Control*, vol. 55, no. 10, pp. 2342–2347, 2010.
- [38] A. S. P., "HIGS-based skyhook damping design of a multivariable vibration isolation system," Master's thesis, Eindhoven University of Technology, 2020.